Optical properties due to electronic transitions in two-dimensional semiconductors $(C_nH_{2n+1}NH_3)_2PbI_4$

Teruya Ishihara, Jun Takahashi,* and Takenari Goto
Department of Physics, Faculty of Science, Tohoku University, Sendai 980, Japan
(Received 5 October 1989; revised manuscript received 12 July 1990)

Optical spectra in the visible and uv regions are investigated in layer-type perovskite compounds $(C_nH_{2n+1}NH_3)PbI_4$ with $n=4$, 6, 8, 9, 10, and 12. The spacing between the PbI_4 layers changes from 15.17 Å for $n=4$ to 24.51 Å for $n=12$. In spite of these different spacings, the optical spectra are almost the same for these compounds, which means that the interaction between the layers is weak. The lowest exciton is located at 2.56 eV at 1.6 K, and its oscillator strength and binding energy are 0.7 per formula unit and 320 meV, respectively. These values are very large compared with those in a three-dimensional analog PbI_2. The large oscillator strength and binding energy can be explained by the small dielectric constant of the alkylammonium "barrier layer," which strengthens the Coulomb interaction between an electron and a hole.

I. INTRODUCTION

In this decade, the unique characteristics of the electronic states in two-dimensional systems are being revealed in both transport and optical phenomena in artificial quantum-well structures. The most prominent feature of the optical properties in the low-dimensional systems is the stability of the exciton. An exciton state in a GaAs bulk crystal is hardly recognizable at room temperature, while in GaAs-$Al_{1-x}Ga_xAs$ multiple quantum wells, it is clearly resolved from the interband absorption.[1] In the two-dimensional limit, the binding energy is known to be four times larger than in the three-dimensional case.[2] In accordance with the shrinkage of the exciton Bohr radius, the oscillator strength becomes larger than that of the bulk exciton.[3]

Moreover, there is a possibility of enhancing the binding energy of an exciton in quantum-well structures. In 1975, Keldysh[4] pointed out that the binding energy of an exciton in a very thin layer medium can be much larger when the surrounding medium has a smaller dielectric constant than that of the well layer. In this case, by virtue of the small dielectric constant, the Coulomb interaction between an electron and a hole is screened less to make them combine more firmly. Sometimes this effect is referred to as "dielectric confinement," although this term does not describe the physics properly. Up to now, this effect has not been yet demonstrated because it is very difficult to create an ideal two-dimensional layer without fluctuation of the thickness in III-V compounds by conventional molecular-beam epitaxy or metal-organic chemical-vapor deposition. It is harder to make an ideal interface with the barrier layers having a smaller dielectric constant.

On the other hand, there are some crystals which have two-dimensional structure by nature. In a single crystal of $(C_nH_{2n+1}NH_3)_2MX_4$, $n=1,2,\ldots,18$; $M=$Cd,Mn,Fe,Cu, ...; $X=$Cl; Br a layer of MX_4 is sandwiched by alkylammonium layers.[5] Let us abbreviate this chemical formula as C_n-MX_4. This unit layer is stacked by the van der Waals interaction to form a single crystal. These materials are candidates of "natural quantum wells" in which the dielectric confinement effect is important because the alkylammonium layers have a wide band gap. They are known in the fields of dielectrics and magnetism. They have the same layer-type perovskite structure as the well-known high-T_c superconductor $La_{2-x}Sr_xCuO_4$. In C_n-MX_4, many studies have concentrated on the sequential structural phase transitions of the alkylammonium chains.[6] The two-dimensional magnetism is also well studied.[7-9] However, only a few papers are related to the optical properties of these materials.[10,11]

Having the motivation stated above, we started to investigate the optical properties in C_n-PbI_4. Because they have absorption peaks in the visible region and the barrier layer has a band gap in the ultraviolet region, the electronic states corresponding to the absorption bands may be confined in the two-dimensional PbI_4 well layers. As for this type of compound, Dolzhenko *et al.*[12] had studied intercalation phenomena in C_9-PbI_4. Recently we[13] reported that the lowest exciton in C_{10}-PbI_4 is very stable.

In this paper, we report the optical spectra of C_n-PbI_4; $n=4,6,8,9,10,12$ in the region of 2.3–5.0 eV. Taking the polarization dependence in the reflection spectra into account, we discuss the origin of the optical transitions. The large binding energy and the oscillator strength of the lowest exciton are explained by the dielectric confinement effect.

In Sec. II experimental procedures are briefly described. In Sec. III the crystal structure is determined by the x-ray-diffraction analysis. The optical spectra in C_{10}-PbI_4 are shown in Sec. IV and the n dependence of the spectra is described in Sec. V. Section VI is devoted to a discussion of the origin of the optical transition and the dielectric confinement, and in Sec. VII a summary is given.

II. EXPERIMENTAL

Single crystals of C_n-PbI_4 were obtained using a silica-gel technique.[14] First, an aqueous solution of $Pb(CH_3COO)_2$, $C_nH_{2n+1}NH_2$, CH_3COOH, and Na_2SiO_3 is prepared in test tubes. After about a week, the mix solution becomes a gel. Then an aqueous solution of KI is poured onto the gel. The I^- ions diffuse into the gel slowly to form C_n-PbI_4 single crystals. One month after the introduction of the I^- ions, squarish platelets with a typical size of $2\times2\times0.1$ mm^3 grow. CH_3COOH is used to control the hardness of the gel, which is essential for the quality of the crystal. C_n-PbI_4 with different n can be grown simply by using different $C_nH_{2n+1}NH_2$ as the starting material for $n=8$, 9, 10, and 12. We could not find any good conditions for growing single crystals of $n=4$ and 6 by this method.

We grew the single crystals with $n=4$ and 6 by evaporation of their aqueous solution.[5] In these cases, we first synthesize iodine salts of alkylamine, then mix with a stoichiometric amount of PbI_2 in water. After filtering the solution, we evaporate it slowly at room temperature. By this method, we obtained single crystals with the size of $1\times1\times0.03$ mm^3. At room temperature, the color of the crystals is orange for $n=4,6,8,9,10$ and yellow for $n=12$.

The crystal structure of C_{10}-PbI_4 was determined by the x-ray-diffraction method. Intensity data were measured at room temperature on a Rigaku automated four-circle diffractometer (AFC5PR) using graphite monochromated Mo$K\alpha$ radiation.

The light sources for absorption and reflection spectra were a halogen lamp and/or a deuterium lamp. Concave mirrors were used to focus the light beams without aberration in the wide wavelength range. The excitation source for the luminescence spectra was a Xe lamp with a uv bandpass filter (Toshiba uv-D1A). The spectra were analyzed by a double monochromator (Jovin-Yvon U1000) with a photomultiplier (Hamamatsu R106). We kept the sample at a given temperature either by immersing it directly into liquid helium or nitrogen, or by mounting it on a temperature-controlled holder.

III. CRYSTAL STRUCTURES

The crystal structure of C_{10}-PbI_4 at room temperature is schematically shown in Fig. 1. The crystal has the layer-type perovskite structure and the space group is D_{2h}^{15} (*Pbca*). A unit cell contains four molecules with the chemical formula of $(C_{10}H_{21}NH_3)_2PbI_4$ and consists of two layers. Lead ions are located on inversion centers and are denoted by open circles in the figure. Iodine ions locate at the corners of the octahedra. Although not shown for the simplicity of the figure, NH_3 heads locate at an A site of the perovskite structure. Alkyl tails extend toward both sides of an inorganic layer. Adjacent octahedra in the same layer rotate in opposite directions by 13° around the c axis.

The distance between Pb and I is 3.20 Å, which compares more favorably with the sum of ionic radii (1.19+2.20=3.39 Å) than to the sum of covalent radii

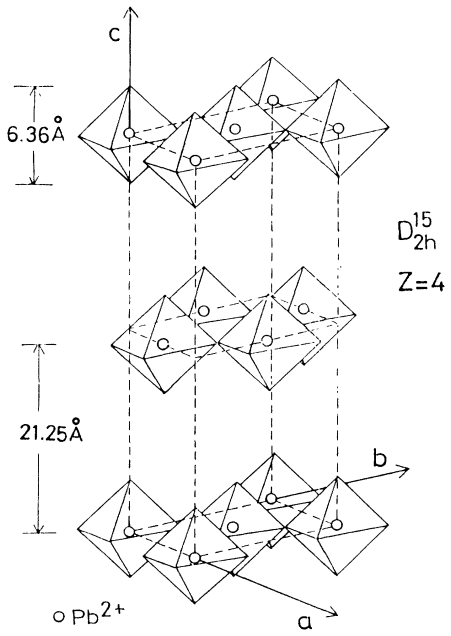

FIG. 1. Schematic unit-cell structure of $(C_{10}H_{21}NH_3)_2PbI_4$. Iodine ions are located at the corners of an octahedron, and an open circle at the center denotes a lead ion. NH_3 heads (not shown) are located at the cavities of octahedra, and alkyl tails (not shown) extend toward both sides of inorganic layers.

(1.54+1.33=2.87 Å). This shows that the chemical bonding in a layer is mainly ionic. The distance between the nearest-neighboring Pb ions is 6.24 Å. The distance between the Pb sheets is 21.25 Å and that between two iodine sheets in a layer is 6.36 Å. Inorganic layer width may be defined as 10.76 Å=6.36+4.40, where the latter is the ionic diameter of an iodine atom.

For $n=9$ and 12, we determined the crystal space group and the lattice constants at room temperature. Obtained values of the lattice constants are summarized in Table I with that for $n=10$. For example, let us see the difference from $n=9$ to 10. In this case, $\delta a/a=-0.75\%$, $\delta b/b=-0.49\%$, and $\delta c/c=+6.87\%$. Thus the change in n gives rise to the change in the interlayer distance. The space group for C_{12}-PbI_4 is supposed to be different from that in C_{10}-PbI_4 and C_9-PbI_4, because the former is in the yellow phase at room temperature. Judging from the extinction rule, the space group for C_{12}-PbI_4 may be C_{2v}^5 (*Pbc*2_1). This group lacks inversion symmetry. The details on the crystal structure will be published elsewhere.[15]

TABLE I. Lattice constants for $(C_nH_{2n+1}NH_3)_2PbI_4$ with $n=9$, 10, and 12.

n	a (Å)	b (Å)	c (Å)
9	9.036	8.710	39.78
10	8.968	8.667	42.51
12	8.882	8.529	49.02

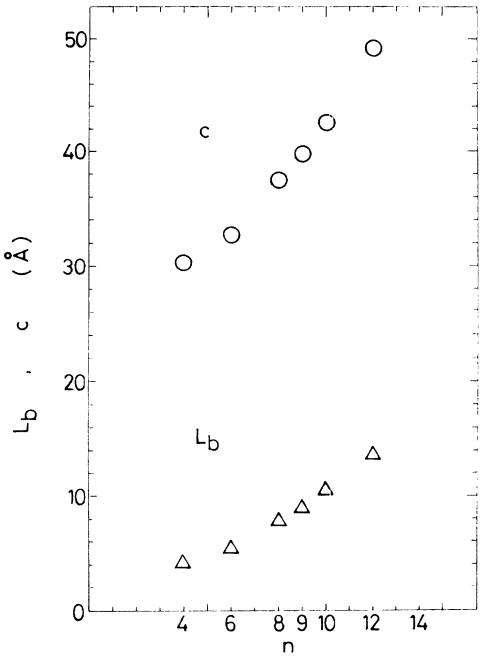

FIG. 2. Lattice constant c (○) and barrier width (Δ) as a function of the number of carbons in an alkylammonium chain in $(C_nH_{2n+1}NH_3)_2PbI_4$. The interlayer distance is $c/2$.

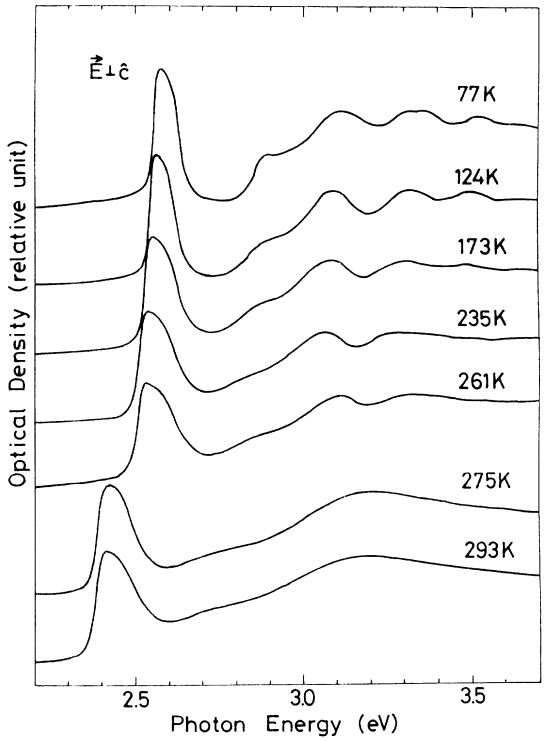

FIG. 3. Optical density spectra in a cleaved thin crystal of $(C_{10}H_{21}NH_3)_2PbI_4$ at several temperatures.

For $n=4$, 6, and 8, we measured the lattice constant c by the use of a powder diffractometer. It is plotted by a circle as a function of n in Fig. 2. Recall that the interlayer distance is one-half of c. As is seen from the figure, we can change the interlayer distance from 14.89 Å for $n=4$ to 24.51 Å for $n=12$, while the well width L_w is a constant of 10.7±0.1 Å. The width of the barrier layer defined as $L_b=c/2-L_w$ is also plotted by a triangle in the figure.

IV. OPTICAL SPECTRA IN C_{10}-PbI_4

Figure 3 shows absorption spectra in C_{10}-PbI_4 at several temperatures in the photon energy region between 2.2 and 3.7 eV. The wave vector of the unpolarized incident light is parallel to the c axis of the crystal. The sample is cleaved several times by means of adhesive tapes. First of all, note that there is a clear absorption peak in the absorption-edge region even at room temperature. This is due to an exciton state, as will be concluded later. The flat-topped shape of these absorption peaks may be caused by the reflection loss for which we did not attempt any correction. The lowest absorption peak at 2.4 eV at 293 K locates in essentially the same position as that at 275 K. At 261 K, it suddenly leaps, however, to the higher-energy side by 100 meV. At this transition, the color of the crystal changes from orange to yellow. Corresponding to this energy shift, the broad band at 3.2 eV at 293 K splits into two bands at 3.1 and 3.3 eV. These spectral changes at this temperature may be caused by a structural phase transition, which is known to occur in C_n-MX_4.[6] The structural phase transition in C_n-PbI_4 is also confirmed by the splitting of Raman lines in the lower-temperature phase, which will be discussed in a separate paper. As the temperature decreases further, the absorption structure becomes clearer, and at 77 K, we can easily see the steplike structure at 2.87 eV. Let us assign it tentatively to two-dimensional band absorption, as its shape is similar to the two-dimensional density of states. Higher members of the exciton series may form quasicontinuum states and merge into the steplike absorption.[2]

Figure 4(a) shows the reflection spectra for an as-grown side face of a C_{10}-PbI_4 single crystal. The upper spectrum is taken for the light with its polarization vector E perpendicular to the c axis, while the lower spectrum is for the parallel configuration. The wave vector of the light k is perpendicular to the c axis for both spectra. Note that there is a large difference between the two spectra. First of all, the exciton structure at 2.55 eV is conspicuous for the $E\perp c$ configuration, while for the $\mathbf{E}\|\mathbf{c}$ configuration, the structure is less intense and sharper. The reflection spectrum for the $\mathbf{k}\|\mathbf{c},\mathbf{E}\perp\mathbf{c}$ configuration is not shown, but it is almost the same as the spectrum for $\mathbf{k}\perp\mathbf{c},\mathbf{E}\|\mathbf{c}$. The peak reflectivity is more than 80%. By the analysis of the Kramers-Kronig transformation, the oscillator strengths of the exciton for the two configurations are found to be 0.7±0.1 and 0.03±0.01, respectively, per formula unit. Such a large oscillator strength is evidence that the peak at 2.55 eV is due to a dipole-allowed direct

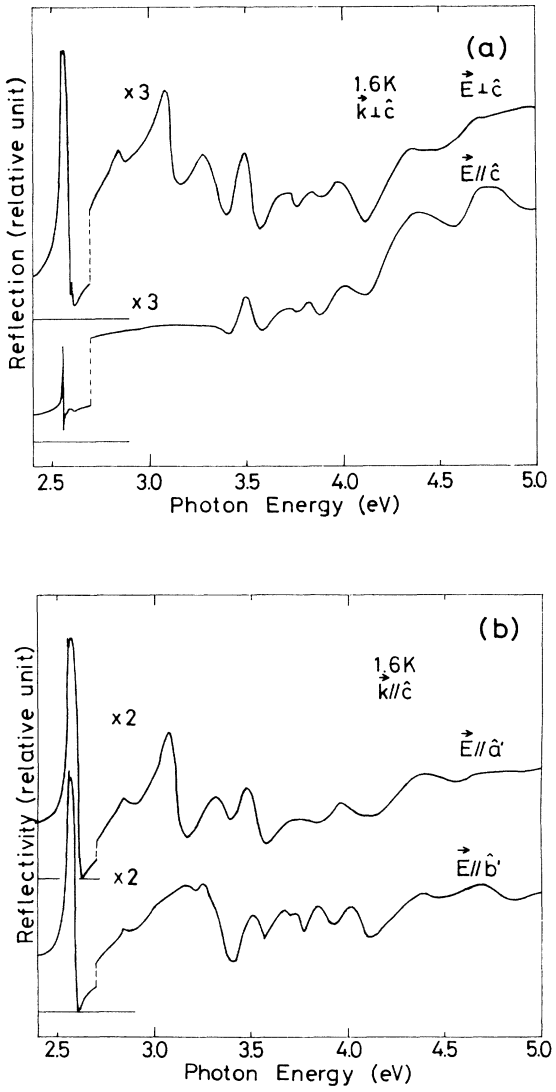

FIG. 4. (a) Reflection spectra in a single crystal of $(C_{10}H_{21}NH_3)_2PbI_4$ for $\mathbf{E}\perp\mathbf{c}$ and $\mathbf{E}\|\mathbf{c}$ configurations at 1.6 K. (b) Reflection spectra in a single crystal of $(C_{10}H_{21}NH_3)_2PbI_4$ for $\mathbf{E}\|\mathbf{a}'$ and $\mathbf{E}\|\mathbf{b}'$ configurations at 1.6 K.

exciton. The structure at 2.554 eV on the main reflection peak for $\mathbf{E}\perp\mathbf{c}$ seems to be due to the interference with the sharp structure of the $\mathbf{E}\|\mathbf{c}$ component at the same energy. At 2.85 eV, there is a kink structure for the $\mathbf{E}\perp\mathbf{c}$ configuration, which corresponds to the step edge in the absorption spectrum.

The structures in the reflection spectra are classified into four groups with respect to their polarization dependences. Group I consists of the structures around 2.55 eV, which are mainly allowed for the $\mathbf{E}\perp\mathbf{c}$ configuration. At 3.1 and 3.3 eV, there are strong bands for the $\mathbf{E}\perp\mathbf{c}$ configuration, but none for the $\mathbf{E}\|\mathbf{c}$ configuration. They belong to group II. Group III are complicated structures between 3.5 and 4 eV, which are allowed for both configurations. Broad bands at 4.3 and 4.7 eV are stronger for the $\mathbf{E}\|\mathbf{c}$ configuration, and are in group IV. These groups will be ascribed to some electronic transitions in Sec. VI A.

Figure 4(b) shows reflection spectra for $\mathbf{k}\|\mathbf{c}$ and $\mathbf{E}\perp\mathbf{c}$ configurations. The two spectra are taken for two orthogonal polarization vectors $\mathbf{a}'$ and $\mathbf{b}'$ which maximize the difference in the spectral position of the reflection minimum at 2.63 eV. The two spectra are rather similar, except for the structure around 3.2 eV. Roughly speaking, we may say that the crystal is uniaxial.

Here we should comment on the effect of irradiation on the reflection spectra. Even weak radiation such as a white light from a 50-W halogen-tungsten lamp changes the reflection spectra irreversibly: the reflection intensity at the exciton peak decreases and the reflection minimum near the longitudinal exciton shifts to the lower-energy side, which indicates the reduction of the oscillator strength. This phenomenon seems to be ascribed to a photochemical reaction at the crystal surface because it is remarkable at higher temperature.

In order to study the stability of the exciton and to obtain information about the electron-lattice interaction, we measured the luminescence spectra at several temperatures. Figure 5 shows the results. First let us see the lowest spectrum taken at 293 K. Note that there is a luminescence band at 2.4 eV, which has almost the same energy as the absorption peak and the reflection structure at this temperature. It is a characteristic feature of this material that the exciton luminescence is observed in the visible region even at room temperature and has no

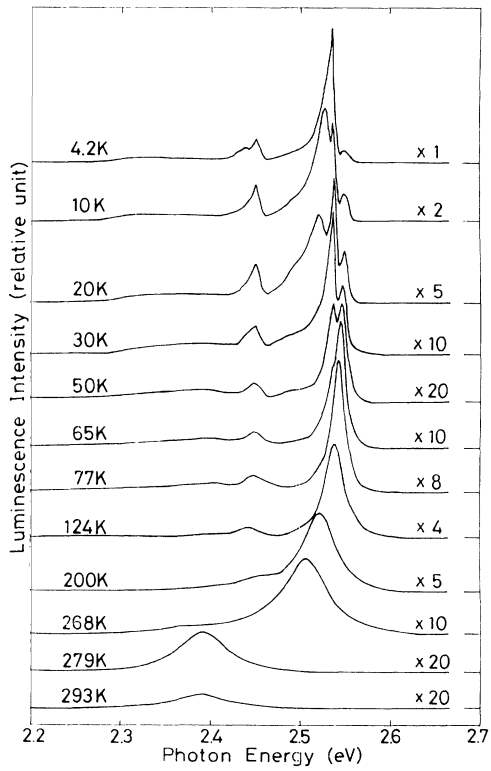

FIG. 5. Photoluminescence spectra in a single crystal of $(C_{10}H_{21}NH_3)_2PbI_4$ at several temperatures.

Stokes shift. Between 279 and 268 K, the luminescence peak shifts discontinously to the higher-energy side, which is again due to the structural phase transition of the crystal. Even in the lower temperature phase, the luminescence peak energy nearly corresponds with that of the absorption. Below 124 K, there is an emission band at 2.45 eV. Because the shape and intensity of the band is sample dependent, this may be ascribed to the luminescence band from a bound exciton trapped deeply at an impurity center. The strongest line at 2.53 eV at 4.2 K decreases its intensity rapidly as the temperature increases. Therefore, this line seems to be due to a shallow bound exciton. The luminescence band due to the free exciton locates at 2.55 eV and is rather weak at 4.2 K. It becomes dominant as the temperature rises, which is a consequence of ionization of the bound excitons. As for the band observed clearly at 10 and 20 K on the lower-energy side of the free-exciton band, it shifts to the lower side immediately when the temperature begins to rise. Its origin is not known at this stage. As strong excitation of the sample also deteriorates the luminescence intensity, the experiments were made under as weak excitation as possible.

Figure 6 shows the integrated intensity of the free-exciton luminescence as a function of the inverse temperature. The luminescence intensity gradually increases as the temperature rises until 170 K and at higher temperatures than 270 K, it decreases as $\exp(E_a/k_BT)$ with $E_a=370\pm50$ meV. This measurement is very difficult because the deterioration of the crystal due to the irradiation is not negligible in the temperature range measured. This results in the large ambiguity of the activation energy. Note that this energy is approximately equal to the energy splitting $\Delta E=320\pm10$ meV between the exciton peak and the step edge in the absorption spectrum. Considering this coincidence, we may regard the steplike absorption as the two-dimensional interband absorption and ΔE as the exciton binding energy hereafter.[16]

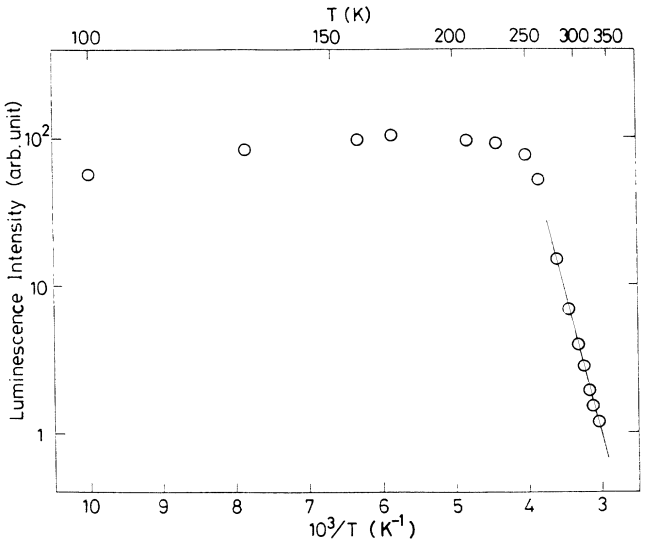

FIG. 6. Temperature dependence of integrated intensity of the free-exciton luminescence in $(C_{10}H_{21}NH_3)_2PbI_4$.

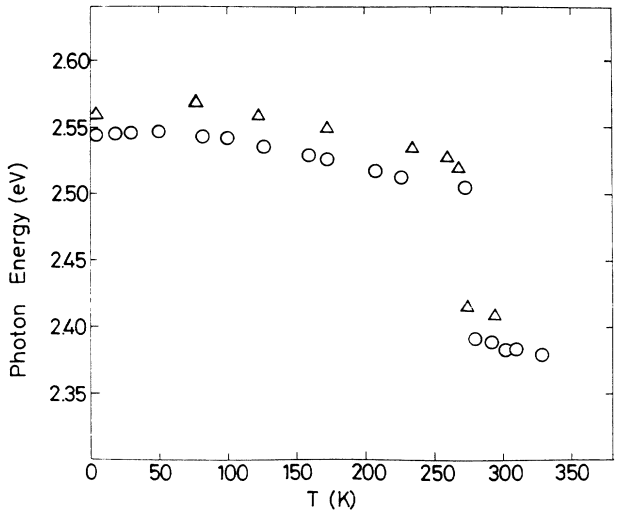

FIG. 7. Energies of absorption (Δ) and luminescence peaks (○) in a single crystal of $(C_{10}H_{21}NH_3)_2PbI_4$ as a function of temperature.

In Fig. 7 the exciton energies determined from the luminescence (Δ) and the absorption (○) spectra are plotted as a function of the crystal temperature. The close correspondence of the two energies at a given temperature shows clearly that the exciton is not self-trapped but free. The slight difference may be ascribed to the reabsorption of light corresponding to the higher-energy-side part in the luminescence band. Above 50 K, the exciton energy decreases as the temperature increases: the coefficient of the energy shift is 2×10^{-4} eV/K. Below 50 K, on the contrary, the exciton energy increases as the temperature increases. The discontinuity at 260 K is obviously distinguished from the usual temperature shift. This is due to the structural phase transition, as was mentioned before.

V. OPTICAL PROPERTIES IN C_n-PbI_4

In this section we show the optical spectra in C_n-PbI_4 in order to see the n dependence of the electronic structure. As in C_{10}-PbI_4, the crystal changes its color at a transition temperature T_c. For $n=4$, 8, 9, 10, and 12, $T_c=250$, 235, 240, 275, and 310 K, respectively. The higher-temperature phase is orange and the lower one is yellow. Because T_c depends strongly on n, and is correlated with the melting temperature of the amine, this transition seems to be related to the structure phase transition caused by rearrangements of the alkylammonium chains.[6] C_6-PbI_4 is exceptional in our experiments. It does not undergo any structural phase transition between room temperature and liquid-helium temperature. Its crystal structure should be studied in the future.

Figure 8 shows the optical density spectra at 1.6 K for $n=4$, 9, 10, and 12 compounds. Note that the spectra are very similar: there is a clear peak at about 2.56 eV, and steplike absorption starts around 2.88 eV. We regard

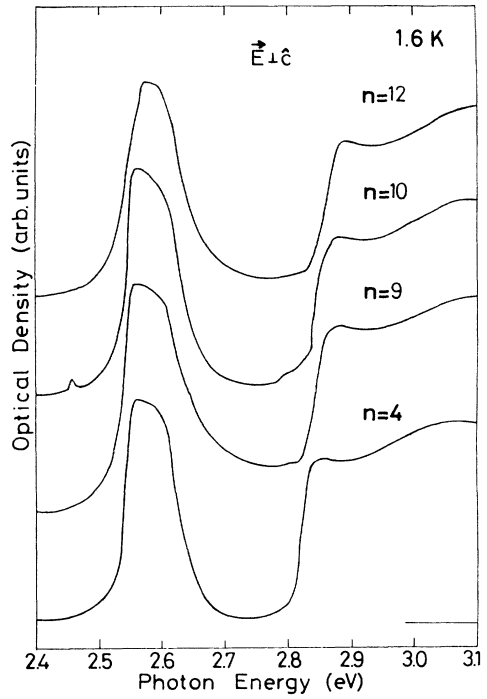

FIG. 8. Optical density spectra in cleaved thin crystals of $(C_nH_{2n+1}NH_3)_2PbI_4$ with $n=4$, 9, 10, and 12 at 1.6 K.

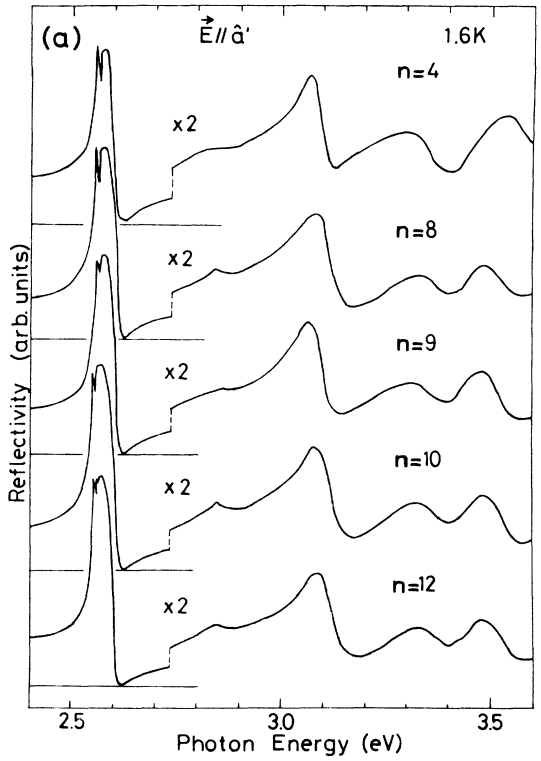

the difference $\Delta E=320\pm30$ meV as the binding energy of the exciton. Although the absorption intensity at the peak of the exciton band and at the step seems to be almost the same, we think that it is superficial. This may come from the inhomogeneity of the thickness in the cleaved sample.

Figures 9(a) and 9(b) show the reflection spectra for $n=4$, 8, 9, 10, and 12 compounds for $\mathbf{E}\|\mathbf{a}'$ and $\mathbf{E}\|\mathbf{b}'$ configurations, respectively. The spectra for different n are very similar, at least in this energy scale. This fact shows that the electronic interaction between the inorganic well layers is very small for C_n-PbI_4 for $n\geq4$.

Figure 10 shows luminescence spectra for $n=4$, 8, 9, 10, and 12 crystals at 1.6 K. The energies of the free-exciton emission are the same in these crystals. Several emission bands in the range of 2.3–2.5 eV are different, which is consistent with our assignment of deeply bound excitons trapped at some impurities.

Figure 11 shows the n dependence of the energy of the longitudinal and transverse excitons. The former is determined from the Kramers-Kronig analysis of the reflection spectrum for the $\mathbf{E}\|\mathbf{a}'(\nabla)$ and $\mathbf{E}\|\mathbf{b}'(\Delta)$ configurations. As for the latter, it is difficult to estimate the transverse exciton energy because of the interference structure and the backface reflection around it. Therefore, we plot the peak energy of the free-exciton luminescence for it by ○. Note that the energy of the longitudinal exciton clearly decreases as n increases, while the transverse exciton energy is essentially the same. Thus the longitudinal-transverse (LT) splitting energy Δ_{LT} de-

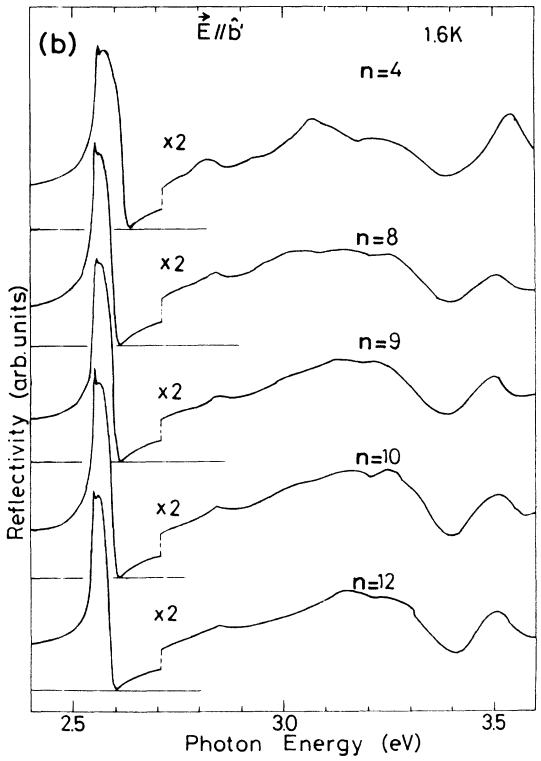

FIG. 9. Reflection spectra in single crystals of $(C_nH_{2n+1}NH_3)_2PbI_4$ with $n=4$, 8, 9, 10, and 12 for (a) $\mathbf{E}\|\mathbf{a}'$ and (b) $\mathbf{E}\|\mathbf{b}'$ configurations at 1.6 K.

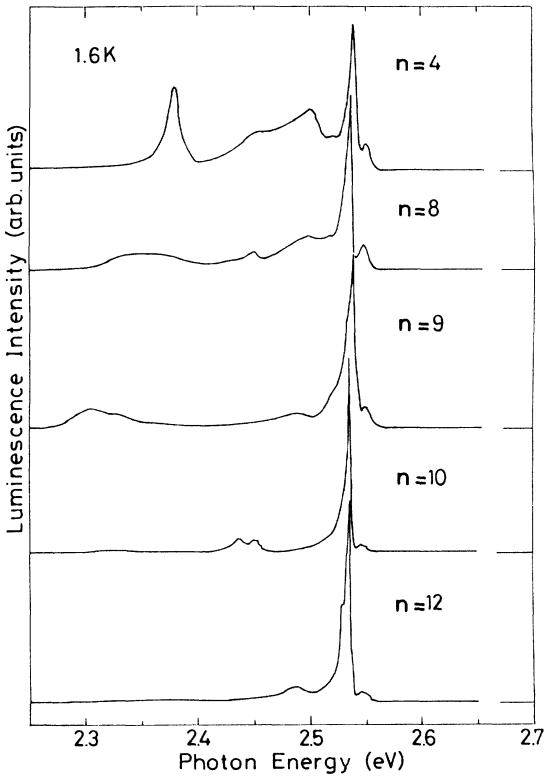

FIG. 10. Photoluminescence spectra in single crystals of $(C_nH_{2n+1}NH_3)_2PbI_4$ with $n=4$, 8, 9, 10, and 12 at 1.6 K.

creases as n increases. The oscillator strength per formula unit can be calculated from Δ_{LT} by the formula

$$f_{exc}=\epsilon_\infty \omega_{LT} m \omega_T V_0 / 2\pi e^2 , \quad (1)$$

where m and e are the mass and the charge of an electron, respectively, ω_{LT} and ω_T are frequencies of the LT splitting and the transverse exciton, respectively. V_0 is the volume of the formula unit, ϵ_∞ is the average high-frequency dielectric constant and

$$\epsilon_\infty=(\epsilon_1 L_w+\epsilon_2 L_b)/(L_w+L_b) , \quad (2)$$

where ϵ_1 and ϵ_2 are the dielectric constant in the wells and the barrier layers, respectively. We choose $\epsilon_1=6.1$ and $\epsilon_2=2.1$, which are the values for PbI_2 (Ref. 17) and $C_nH_{2n+1}NH_2$,[18] respectively. The oscillator strength of the lowest exciton in C_n-PbI_4 is plotted by ∇ ($\mathbf{E}\|\mathbf{a}'$) and $\Delta(\mathbf{E}\|\mathbf{b}')$ as a function of n in Fig. 12. Although the oscillator strength appears to decrease as n increases, we are not sure that it actually does because ϵ_∞ is estimated from the simple model. At this state, we can say that the oscillator strength of the lowest exciton state for the $\mathbf{E}\|\mathbf{a}'$ configuration is 0.7 ± 0.2.

From the temperature dependence of the luminescence intensity of the free-exciton band, we estimate the activation energy E_a, which is shown by □ in Fig. 12. The value for $n=12$ is determined at the yellow phase, while it is determined at the orange phase for the other n. E_a is in the range between 330 and 430 meV. The energy separation ΔE between the exciton absorption and the step-like absorption edge is also shown in Fig. 12 for comparison. We may say that the quenching of the exciton luminescence in these materials is dominated by the thermal excitation to the continuum state above 2.86 eV.

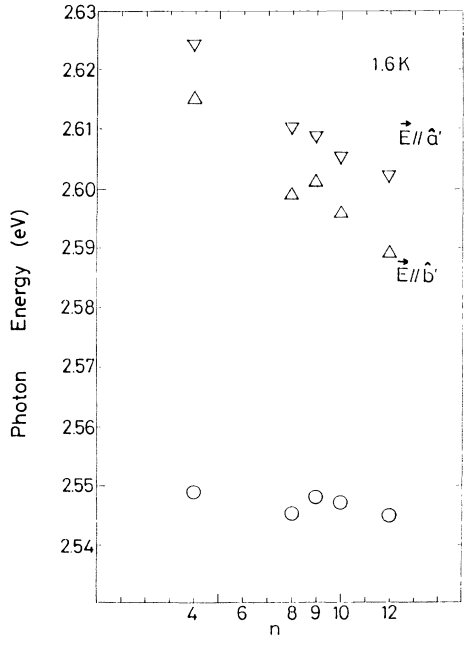

FIG. 11. The energies of the longitudinal (∇, $\mathbf{E}\|\mathbf{a}'$; Δ, $\mathbf{E}\|\mathbf{b}'$) and transverse (○) excitons in $(C_nH_{2n+1}NH_3)_2PbI_4$ at 1.6 K.

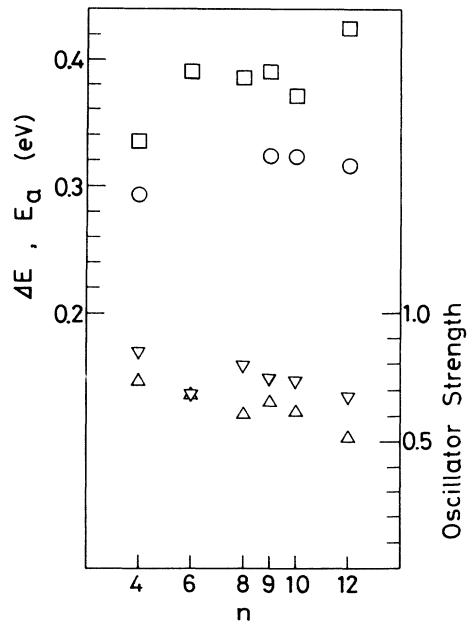

FIG. 12. Oscillator strength of the lowest exciton for $\mathbf{E}\|\mathbf{a}'$ (∇) and $\mathbf{E}\|\mathbf{b}'$ (Δ) configurations, the activation energy E_a (□) and the separation energy ΔE (○) in $(C_nH_{2n+1}NH_3)_2PbI_4$.

VI. DISCUSSION

A. Assignment of optical transition

Because alkylammonium iodide is optically transparent in the visible region,[19] the optical transitions observed in our experiments are ascribed to those in PbI_4^{2-} well layers. Considering that the Pb-I distance in C_n-PbI_4 is approximately equal to the sum of ionic radii, as was shown in Sec. III, it seems that the chemical bondings in the well layer are mainly ionic. Let us take the atomic excitation picture as the starting basis. In this picture, the electronic configuration in the ground state is $(6s)^2$ for Pb^{2+} and $(5p)^6$ for I^-. The lowest excited state is a cationic excitation in which Pb^{2+} is excited to $(6s)(6p)$, leaving the I^- unchanged. This configuration will have lower energy than the configuration Pb:$(6s)^2(6p)^2$; I:$(5p)^5$, on account of more Madelung energy. The anionic excitation will have higher energy because I^- has a closed-shell configuration in the ground state. These situations may be different from that in C_n-$CdCl_4$, where Cd^{2+} has a closed-shell configuration.[11]

The first excited state in the cationic excitation model has threefold degeneracy, which lifts on application of the crystal field and spin-orbit interaction. This situation is similar to that in PbI_2, which is one of the well-known layer-type semiconductors.[20] Although PbI_2 has many polytype structures, we will discuss $2H$-PbI_2 for simplicity.

The space group of $2H$-PbI_2 is D_{3d}^3 and the number of formula units un a unit cell $Z=1$. As for this crystal, the semiempirical pseudopotential band calculation has been carried out.[21] A direct gap at the A point is the lowest one. Because of the D_{3d} crystal field and the spin-orbit interaction, the threefold degeneracy in the conduction band lifts into three bands, A, B, and C. Corresponding to the three conduction bands, the optical transitions from the topmost valence band, which consists mainly of the Pb $6s$ function, are named A, B, and C bands. These bands have different polarization dependences. The lowest transition A (2.498 eV) is mainly allowed for the $\mathbf{E}\perp\mathbf{c}$ configuration, while the uppermost transition C (3.94 eV) is mainly allowed for $\mathbf{E}\parallel\mathbf{c}$. The B band (3.31 eV) is allowed only for $\mathbf{E}\perp\mathbf{c}$. The ratio in the oscillator strength of $\mathbf{E}\perp\mathbf{c}$ to $\mathbf{E}\parallel\mathbf{c}$ configurations, which is 4:1 for the A band, depends on the strength ratio of the crystal field to spin-orbit interaction. The energy splittings among A, B, and C bands also depend on the ratio. The binding energy for the lowest exciton state in PbI_2 was historically controversial.[22–24] We adopt 30 meV (Ref. 23) for the binding energy and 19 Å (Ref. 24) for the exciton Bohr radius tentatively in this paper.

Now let us go back to Fig. 4. We easily see that the groups I, II, and IV in the reflection spectra correspond to the A, B, and C transitions. The complicated structures in group III may correspond to a kink at 3.6 eV in PbI_2.[20] These correspondences demonstrate that the origins of these optical transitions are essentially the same, that is, the cationic excitations of the lead ions. Furthermore, the similarity in the temperature coefficient of the exciton energy in C_n-PbI_4 and in PbI_2 (Ref. 25) may show the similarity in the electronic states. The band splittings in each band in C_n-PbI_4 may be caused by band folding, because its unit cell contains four formula units. A band calculation for C_n-PbI_4 is necessary in order to further discuss its optical transitions.

B. Mechanism of large binding energy and oscillator strength

As discussed above, the optical transitions in C_n-PbI_4 are similar to that in PbI_2. But there are great differences on the lowest exciton state. Although the formation energies of two excitons are similar, their binding energies and oscillator strengths are quite different: 320 meV and 0.7 for C_n-PbI_4, and 30 meV (Ref. 23) and 0.017 (Ref. 26) for PbI_2. What makes the two excitons so different?

It is well known that a two-dimensional exciton has a binding energy four times larger than that of a corresponding three-dimensional exciton.[2] Such a small enhancement does not explain the much larger binding energy of an exciton in C_n-PbI_4. Keldysh,[4] however, discussed the Coulomb interaction between an electron and a hole in a layer surrounded by a medium with a smaller dielectric constant. In this circumstance, on account of less screening in the surroundings, the binding energy of an exciton can be much larger. This is just the case with C_n-PbI_4, where the dielectric confinement effect is quite large: the well width is extremely thin (11 Å which is about one-half of the exciton Bohr radius in PbI_2) and the dielectric constants are very different (6.1 for well layers[17] and 2.1 for barrier layers[18]).

Hanamura *et al.*[27] calculated the exciton binding energy as a function of the ratio in the dielectric constants of the well to the barrier layers. From their calculation curve, we deduce that the exciton binding energy in C_n-PbI_4 should be about seven times larger than PbI_2 that is, 210 meV. The agreement is satisfactory, taking the ambiguity of the binding energy in PbI_2 into account. Furthermore, the Bohr radius of the exciton in C_n-PbI_4 can be deduced from their calculation to be 0.6 times that in PbI_2, or 11 Å, which is large enough to cover the nearest-neighbor lead ions 6.24 Å distant. Thus the lowest exciton in C_n-PbI_4 is a Wannier exciton with a small radius in this model. The oscillator strength can be calculated using a formula,

$$f_{\mathrm{exc}}=2fS_0/\pi a_{2\mathrm{D}}^2 , \tag{3}$$

for a two-dimensional exciton. For C_{10}-PbI_4, the unit-cell area $S_0=39$ Å^2 and the two-dimensional Bohr radius $a_{2\mathrm{D}}=11$ Å. The interband oscillator strength f is supposed to be the same as that in PbI_2 and is estimated to be 3.4 from the relation

$$f_{\mathrm{exc}}(PbI_2)=fV_0/\pi a_{3D}^3=0.017 , \tag{4}$$

where the unit-cell volume $V_0=126$ Å^3 and $a_{3\mathrm{D}}=19$ Å. From Eqs. (3) and (4) f_{exc} in C_{10}-PbI_4 is calculated to be 0.69, which agrees with the experimental value 0.7 quite well.

Thus the large binding energy and oscillator strength in C_n-PbI_4 can be explained by the dielectric confinement

model, assuming that the exciton reduced mass, the interband oscillator strength, and the dielectric constant in the well are the same as those in PbI_2. In order to verify the dielectric confinement effect, experimental estimation of the exciton mass is important. Studying the properties of the exciton for the compounds with smaller barrier width will also be useful for the verifications. These experiments are in progress.

VII. CONCLUSIONS

Absorption, reflection, and luminescence spectra in C_n-PbI_4 with $n=4$, 6, 8, 9, 10, and 12 have been measured. Our results are summarized as follows.

(1) C_n-PbI_4 has layer-type perovskite structure. The interlayer distance increases with n, while the well thickness is constant.

(2) The optical spectra are anisotropic and are almost n independent. The optical transition in C_n-PbI_4 comes from the 6*s* to 6*p* transition in Pb^{2+}, as in the case of PbI_2.

(3) The lowest exciton is free and locates at 2.56 eV for the yellow phase and at 2.4 eV for the orange phase.

(4) The lowest exciton is stable even at room temperature. The binding energy is about 320 meV and the oscillator strength per formula unit is 0.7.

(5) The large binding energy and oscillator strength in the lowest excitation state in C_n-PbI_4 may be explained by the dielectric confinement effect.

ACKNOWLEDGMENTS

The authors would like to thank Professor Y. Maruyama and Dr. T. Inabe (Institute for Molecular Science) for teaching us a method of synthesizing C_n-PbI_4 single crystals, and Dr. C. Kabuto, Professor M. Shimoi (Tohoku University), and Professor H. Miyamae (Josai University) for helping us to analyze the crystal structures. Thanks are also due to Professor E. Hanamura (University of Tokyo) and Dr. T. Yoshinari (Yamagata University) for useful discussions. This work is partially supported by a Grant-in-Aid for Scientific Research from the Ministry of Education, Science and Culture of Japan.

---

*Present address: Nippon Steel Corporation, R&D Laboratories I, 1618 Ida, Nakahara-ku, Kawasaki, 211 Japan.

[1]D. A. B. Miller, D. S. Chemlar, D. J. Eilenberger, P. W. Smith, A. C. Gossard, and W. T. Tsang, Appl. Phys. Lett. **41**, 679 (1982).

[2]M. Shinada and S. Sugano, J. Phys. Soc. Jpn. **21**, 1936 (1966).

[3]Y. Masumoto and M. Matsuura, Phys. Rev. B **32**, 4275 (1985).

[4]L. V. Keldysh, Pis'ma Zh. Eksp. Teor. Fiz. **29**, 716 (1979) [JETP Lett. **29**, 658 (1979)].

[5]H. Arend, W. Huber, F. H. Mischgofsky, and G. K. Richter-van Leeuwen, J. Cryst. Growth **43**, 212 (1978).

[6]R. Kind, Ferroelectrics **24**, 81 (1980).

[7]L. J. de Jongh, A. C. Botterman, F. R. de Boer, and A. R. Miedema, J. Appl. Phys. **40**, 1363 (1969).

[8]G. Heger, E. Henrich, and B. Kanellakopulos, Solid State Commun. **12**, 1157 (1973).

[9]P. Bloembergen, Physica **85**, 51 (1977).

[10]N. Watanabe, N. Kojima, T. Ban, and I. Tsujikawa, J. Phys. C **21**, 4795 (1988).

[11]T. Yoshinari, T. Nanba, S. Shimanuki, M. Fujisawa, T. Matsuyama, M. Ikezawa, and K. Aoyagi, J. Phys. Soc. Jpn. **58**, 2276 (1989).

[12]Yu. I. Dolzhenko. T. Inabe, and Y. Maruyama, Bull. Chem. Soc. Jpn. **59**, 563 (1986).

[13]T. Ishihara, J. Takahashi, and T. Goto, Solid State Commun. **69**, 933 (1989).

[14]H. K. Henish, *Crystal Growth in Gels* (Pennsylvania State University Press, Pennsylvania, 1970).

[15]T. Ishihara, J. Takahashi, and M. Shimoi (unpublished).

[16]In Ref. 13 we regarded E_a as the exciton binding energy. It is difficult, however, to determine E_a uniquely from the experiment without any ambiguity. In this paper, we choose ΔE for the exciton binding energy in order to make the discussion clearer. The discussions in Ref. 13 are essentially correct because the difference between ΔE and E_a is not so large.

[17]G. Lucovsky, R. M. White, W. Y. Liang, R. Zallen, and Ph. Schmid, Solid State Commun. **18**, 811 (1976). In Ref. 13 we used the static dielectric constant to estimate the dielectric confinement effect. We should, however, use the high-frequency dielectric constant because the binding energy is much larger than the energy of the optical phonon.

[18]*CRC Handbook of Chemistry and Physics*, 63rd ed. (Chemical Rubber Company, Boca Raton, FL, 1983). The high-frequency dielectric constant of the barrier layers is estimated from the refractive index of $C_{10}H_{21}NH_2$.

[19]The absorption edge in $C_{12}H_{25}NH_2$ locates at 5.5 eV at room temperature.

[20]C. Y. Fong and M. Schlüter, in *Electrons and Phonons in Layered Crystal Structures*, edited by T. J. Wieting and M. Schluter (Reidel, Holland, 1979), p. 229.

[21]I. Ch. Schlüter and M. Schlüter, Phys. Rev. B **9**, 1652 (1974).

[22]Ch. Gähwiller and G. Harbeke, Phys. Rev. **185**, 1141 (1969).

[23]Le Chi Tanh, C. Depeursinge, F. Levy, and E. Mooser, J. Phys. Chem. Solids **36**, 699 (1975).

[24]Y. Nagamune, S. Takeyama, and N. Miura, Phys. Rev. B **40**, 8099 (1989).

[25]R. Kleim and F. Raga, J. Phys. Chem. **30**, 2213 (1969).

[26]G. Harbeke, F. Bassani, and E. Tosati, in *Proceedings of the International Conference on the Physics of Semiconductors* (Polish Scientific, Warsaw, 1972), p. 163.

[27]E. Hanamura, N. Nagaosa, M. Kumagai, and T. Takagahara, Material Sci. Eng. B **1**, 255 (1988).